Topography of high- and low-index GaAs surfaces

R. Nötzel, L. Däweritz,* and K. Ploog†
Max-Planck-Institut für Festkörperforschung, D-7000 Stuttgart 80, Federal Republic of Germany
(Received 26 December 1991; revised manuscript received 18 May 1992)

We have investigated the surface structure of the nonsingular (331), (311), (211), and (210) GaAs surfaces and of the singular (110) and (111) GaAs surfaces during molecular-beam epitaxy. Reflection high-energy electron diffraction directly reveals the formation of periodically arranged macrosteps with spacings and heights in the nanometer range. Nonsingular planes break up into singular surface configurations, whereas the singular surfaces transform into vicinal planes. Surface reconstruction plays an important role in the stabilization of terrace and step widths. The surface structures give rise to lateral confinement effects, which drastically changes the electronic properties of GaAs/AlAs multilayer structures.

I. INTRODUCTION

The atomic arrangement of solid surfaces on the microscopic scale is an important scientific problem and plays an essential role in a number of processes, including crystal growth, epitaxy, and etching. The starting point is the determination of the equilibrium surface configuration which is governed by the surface free energy.[1] Considering the surface energy, crystal faces are classified into three types: singular ones, which coincide with planes of high symmetry (low Miller index surfaces) corresponding to local minima in surface energy, vicinal ones which lie in the vicinity of singular planes, and all other nonsingular planes.[2] Three important groups of nonsingular surfaces are distinguished which lie on the sides of the unit stereographic triangle of the cubic crystal with the singular (100), (110), and (111) planes assigned with the corners (Fig. 1).[2] The planes of each of these groups can be constructed from steps made up of varying proportions of surface configurations corresponding to the singular planes of the adjacent corners.[3] Typical representatives possessing the general characteristics of each of these groups are the (331) plane between (110) and (111), the (311) plane between (100) and (111), and the (210) plane between (100) and (110).[4] Simple theoretical models, taking into account only the interaction between nearest atoms, have shown that in the case of ideal lattices nonsingular planes are unstable.[2] This finding leads to the idea that planes with high surface energy break up into faces corresponding to planes with lower surface energy forming distinct ordered surface structures on a nanometer scale which represent the equilibrium configuration. These surface structures give rise to lateral confinement effects in GaAs/AlAs multilayer structures and hence provide a unique means to directly synthesize quantum-wire and quantum-dot structures during epitaxial growth.

In this paper we report on surface structures observed on the nonsingular (331), (311), (211), and (210) surfaces and on the singular (110) and (111) surfaces during molecular-beam epitaxy (MBE). The analysis of reflection high-energy electron diffraction (RHEED) directly shows the existence of periodically arranged steps with spacings and heights on a nanometer scale. Generally we observe the breaking up of nonsingular surfaces into singular surface configurations, whereas the singular surfaces transform into vicinal planes. In Fig. 1 the investigated planes are marked on the unit stereographic triangle. The arrows indicate the observed transformation of these planes into surface configurations corresponding to a variety of different planes on the stereographic triangle. In order to give an idea of the geometrical situation, a cross section of the host GaAs crystal viewed along the $[01\bar{1}]$ direction is shown in Fig. 2 where the surface configurations corresponding to the (100), (011), (111), (211), and (311) planes can be seen in $[01\bar{1}]$ projection. The resulting surface structures are found to be composed of multiples of units having these surface configurations [in the following referred to as the number of (*hkl*) surface configurations] and to be stabilized by the (2×2) surface reconstruction of the singular (111) plane.

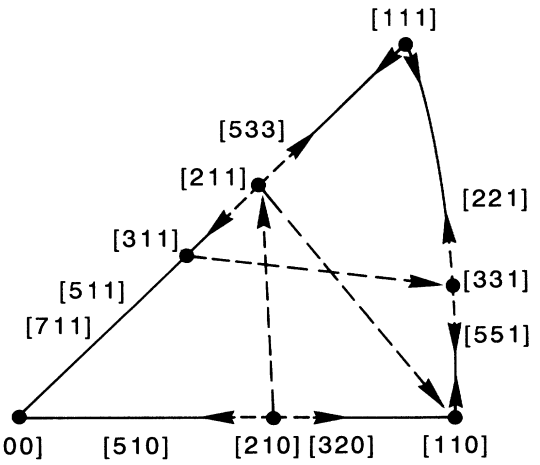

FIG. 1. Unit stereographic triangle. The investigated planes are marked. The arrows indicate the observed transformation of the planes.

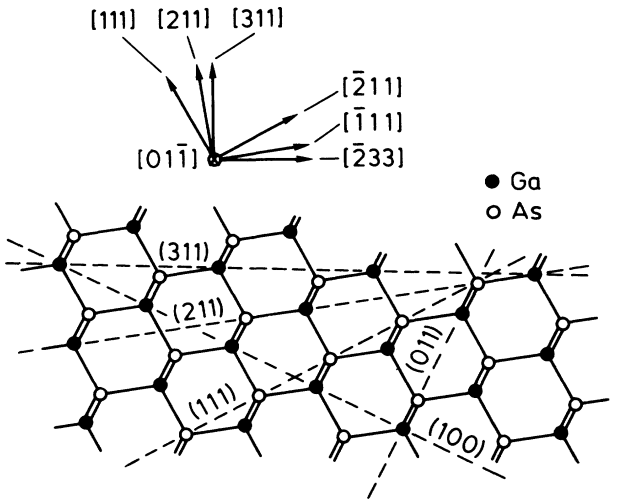

FIG. 2. Cross section of the host GaAs crystal viewed along [01$\bar{1}$]. The (100), (011), (111), (211), and (311) planes are indicated.

Periodic step arrays are formed on the (331) and (110) surfaces, periodic channels on the (311) surface, symmetric pyramids on the (111) surface, asymmetric pyramids in one direction on the (211) surface, and asymmetric pyramids in two directions on the (210) surface. These surface structures indeed result in the direct formation of quantum-wire and quantum-dot structures during MBE which is manifested in the electronic properties of GaAs/AlAs multilayer structures.

The paper is organized as follows. The sample preparation and experimental setups used for our investigations are described in Sec. II. Section III is devoted to the results of the RHEED studies. In Sec. IV we briefly describe the electronic properties of GaAs/AlAs multilayer structures grown on the various surfaces. Finally in Sec. V we summarize our results.

II. SAMPLE PREPARATION AND EXPERIMENTAL SETUPS

The differently oriented GaAs substrates were cleaned in ultrasonically stirred concentrated sulfuric acid. After carefully rinsing in water and blowing dry with nitrogen gas the substrates were heated to 300 °C in dust-free air to passivate the surface with an oxide film.[5] Compared to the commonly used method of preparing GaAs substrates by chemical etching in a $H_2SO_4/H_2O_2/H_2O$ mixture, our method has the advantage of a negligible etching rate which allows the preparation of substrates with different crystallographic orientations in a comparable manner. After the cleaning procedure, the substrates were transferred into the RIBER 2300 MBE growth chamber where the surface oxide was thermally desorbed at 580 °C. GaAs layers and GaAs/AlAs multilayer structures were grown at a growth rate of 1 μm/h for GaAs and 0.5 μm/h for AlAs. The As_4/Ga flux ratio was 5. The growth was monitored by RHEED using a 30-kV beam from a RIBER CER-1050 electron gun at 1° glancing angle incidence. The measurement system consisted of video camera, video recorder, and image processing system. Photoluminescence (PL) and photoluminescence excitation (PLE) measurements were performed with the samples mounted in an optical He-flow cryostat. Light from a broadband 600-W halogen lamp dispersed by a 0.5-m double-grating monochromator served as an excitation source. The luminescence was analyzed by a 1-m single-grating monochromator and detected by a cooled GaAs photomultiplier operating in the photon-counting mode.

III. RHEED STUDIES

The RHEED technique has the advantage of directly imaging the reciprocal space of surface structures projected along the direction of observation. In order to facilitate the discussion of the observed RHEED patterns, we briefly specify the reciprocal space of ordered surface structures.[6,7] The typical asymmetric reciprocal space of periodic step arrays with only one step sense (upward or downward) is presented in Fig. 3(a). The lateral periodicity l and the step height h are deduced from the horizontal splitting of the streaks into slashes and from the length of the streaks normal to the surface, respectively. The step height h as defined in Fig. 3(a) enables a unified description of the height of the surface structures ob-

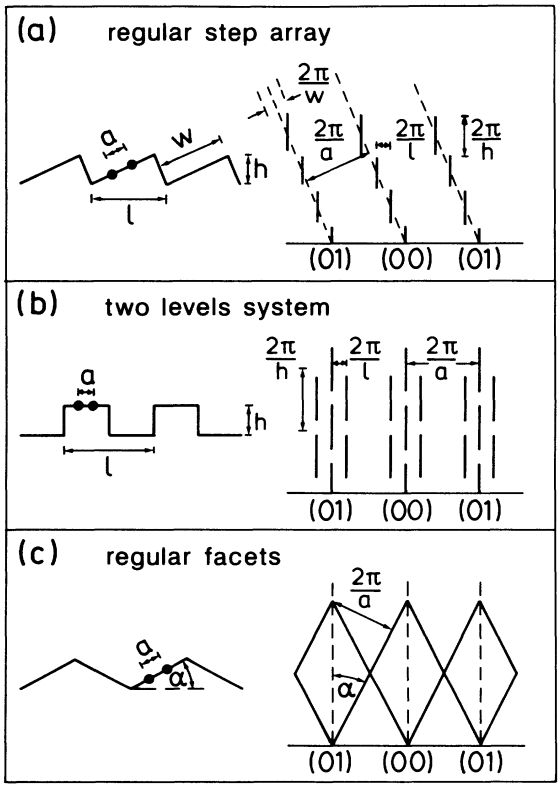

FIG. 3. Periodic surface structures with their representation in reciprocal space. (a) regular step array, (b) two-level system, and (c) regular facets.

served in this work representing transitions between stepped and faceted surfaces with comparable terrace and step widths. The commonly used definition of the step height $d=h/\cos\alpha$, where α is the inclination of the terrace to the nominal surface,[7] is not appropriate in this case for nonperpendicular terraces and steps. Fluctuations of the terrace width result in broadening and also lengthening of the slashes leading to deviations for the evaluated step height. The degree of ordering of the surface structure, i.e., the average domain size of ordering, is estimated from the full width at half maximum (FWHM) of the slashes. The lattice constant a of the terrace plane is determined from the separation of the corresponding integral order streaks which are oriented along the lines connecting the intensity maxima of the slashes (dashed lines). The terrace width w is estimated from the FWHM of the streaks corresponding to the terrace planes. The reciprocal space of a two-level system with symmetrically arranged upward and downward steps [Fig. 3(b)] exhibits streaks which are split alternately into satellites and along their length. Intensity maxima of the satellites correspond to intensity minima of the integral order streaks and vice versa. The lateral periodicity l and step height h are deduced from the separation of the satellites and the splitting along the streaks, respectively. The reciprocal space of regular facets exhibits a periodic arrangement of tilted streaks [Fig. 3(c)]. The tilt angle α of the facet plane with respect to the nominal surface is determined from the tilt angle of the streak to the surface normal. The lattice constant a of the facet plane is determined from the streak separation.

A. RHEED studies of nonsingular surfaces

The RHEED pattern of the (331) surface observed along $[1\bar{1}0]$ [Fig. 4(a)] reveals a regular step array with the step edges running along $[1\bar{1}0]$. This RHEED pattern is obtained after the deposition of several GaAs monolayers at temperatures below 550 °C and is stable during growth. When heating the substrate above 550 °C, the surface roughens and forms irregular macroscopic facets which is indicated by a spotty RHEED pattern along $[1\,\bar{1}\,\bar{0}]$ with an arrangement of disordered, nonperiodic tilted streaks connected with the reflection spots. This faceted surface is maintained during cooling below 550 °C. The regular step array is reestablished after again depositing several GaAs monolayers. The lateral periodicity l and the step height h amount to $l=18$ Å and $h=3.5$ Å. The terrace width w is estimated to $w=12$ Å. The observed lattice constant a of the terrace plane of 5.7 Å ($\hat{=}a_{[100]}$) identifies the (110) surface configuration in $[1\bar{1}0]$ projection. The average domain size is estimated to be 100 Å or more which is in the range of the transfer width determined for our RHEED system.[6] Observation along $[\bar{1}\,\bar{1}6]$ [Fig. 4(b)] shows a streaky RHEED pattern in agreement with the step edges along $[1\bar{1}0]$. Hence, the (331) surface breaks up into a regular step array of 2.6-Å height ($\hat{=}2d_{[331]}$) with (110) terrace planes of 11-Å width ($\hat{=}2a_{[100]}$), and (111) steps of 6.9-Å width ($\hat{=}2a_{[211]}$) [Fig. 4(c)].

The RHEED pattern of the (311) surface reveals a pronounced streaking with the electron beam along $[01\bar{1}]$ [Fig. 5(a)] indicating a high density of steps along the perpendicular $[\bar{2}33]$ direction. Along $[\bar{2}33]$, we observe the RHEED pattern of an almost perfect two-level system [Fig. 5(b)]. The high degree of ordering manifests itself in the cancellation of the 00 streak intensity for maximum intensity of the satellites.[7] The surface is found to be stable from 680 °C down to room temperature. The lateral periodicity l and the step height h amount to $l=32$ Å and $h=10$ Å. As a consequence, the (311) surface is built up from two sets of $(33\bar{1})$ and $(\bar{3}1\bar{3})$ facets along $[\bar{2}33]$ corresponding to upward and downward steps of 10-Å height ($\hat{=}6d_{[311]}$) and (311) terrace planes of 4-Å width ($\hat{=}a_{[110]}$) [Fig. 5(c)]. From the above discussion of the [331] orientation, the {331} facets are assumed to be stabilized by a terrace plane comprising two (110) surface configurations and a step comprising two (111) surface configurations.

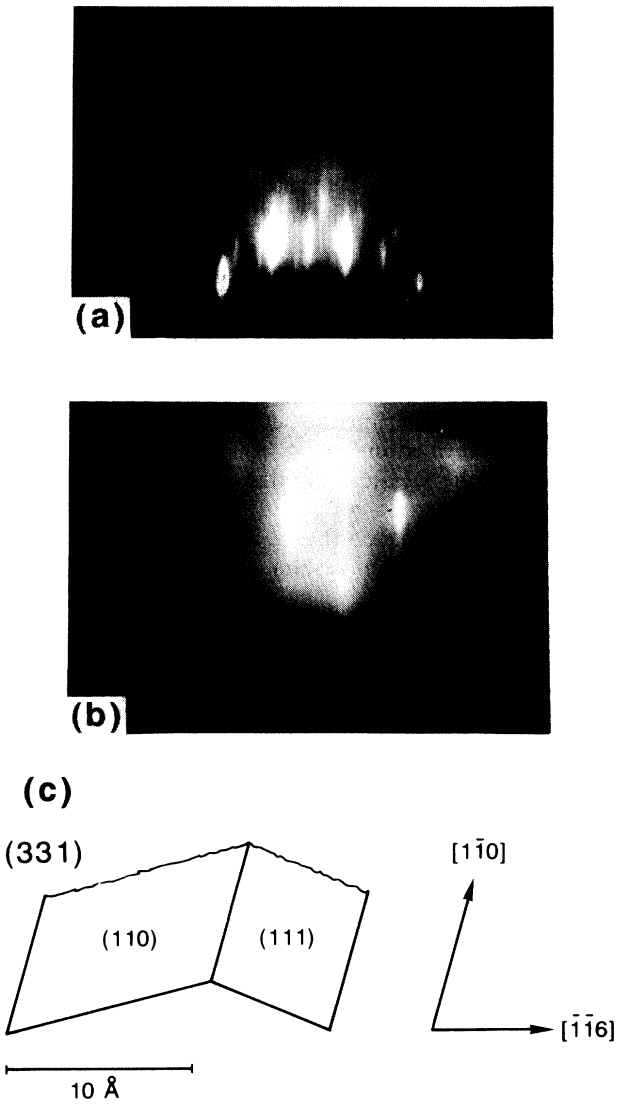

FIG. 4. Reflection high-energy electron diffraction (RHEED) pattern of the GaAs (331) surface taken (a) along $[1\,\bar{1}0]$ and (b) along $[\bar{1}\,\bar{1}6]$. (c) Schematic of the stepped surface.

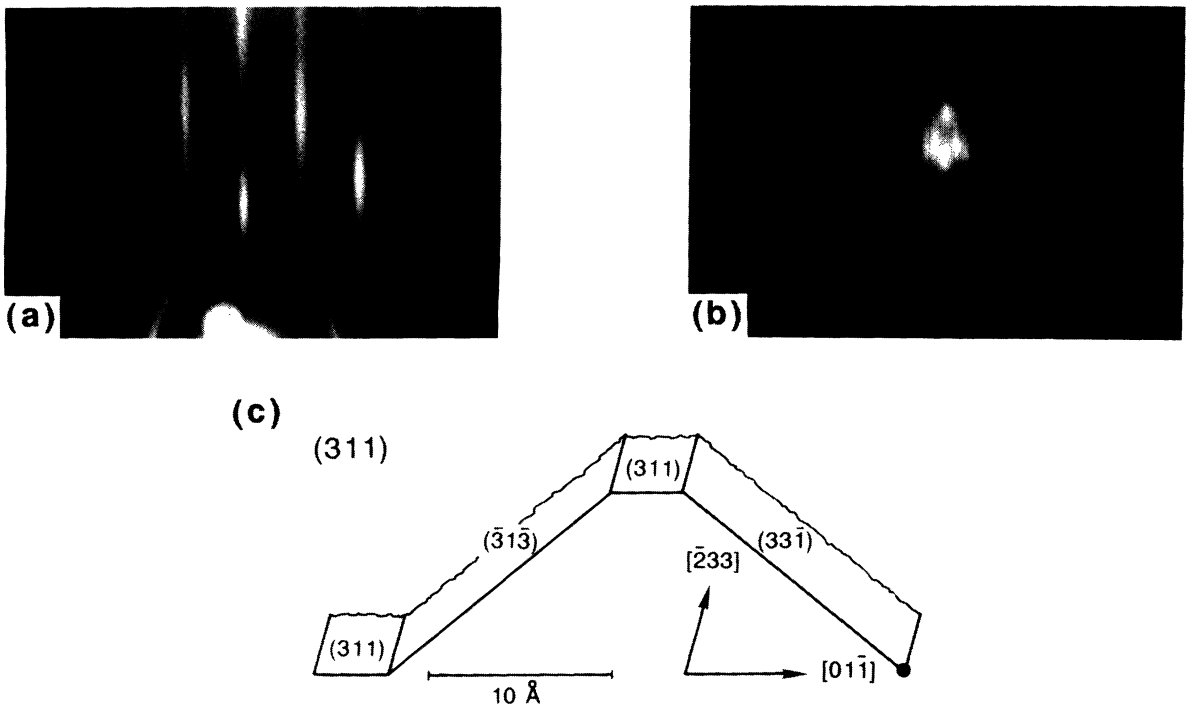

FIG. 5. Reflection high-energy electron diffraction (RHEED) pattern of the GaAs (311) surface taken (a) along $[01\bar{1}]$ and (b) along $[\bar{2}33]$. (c) Schematic of the stepped surface.

The RHEED pattern of the (211) surface observed along the $[01\bar{1}]$ azimuth reveals a regular step array with the step edges along $[01\bar{1}]$ [Fig. 6(a)]. Along the perpendicular $[\bar{1}11]$ azimuth [Fig. 6(b)] the RHEED pattern shows an array of regular facets. The surface undergoes a reversible transition from the regular faceted surface to the flat surface below 590 °C. The transition occurs continuously over a temperature range between 590 °C and 550 °C [Figs. 6(c) and 6(d)]. The flat surface observed along $[\bar{1}11]$ [Fig. 6(d)] and along $[01\bar{1}]$ exhibits diffuse streaks indicating a pronounced degree of disorder. The faceted surface is stable during growth above 600 °C. The lateral periodicity l and the step height h of the regular step array amount to $l=9.8$ Å and $h=3.6$ Å. The terrace width w is estimated to $w=9.6$ Å. The (111) surface configuration in $[01\bar{1}]$ projection of the terrace plane follows from the lattice constant $a=3.4$ Å ($\triangleq a_{[211]}$). The average domain size amounts to about 70 Å. The regular facets observed along $[\bar{1}11]$ correspond to (110) surface configurations as evaluated from the tilt angle $\alpha=30°$. As a consequence, the (211) surface comprises two sets of $\{110\}$ facets along $[\bar{1}11]$ and alternating (111) terrace planes of 6.9-Å width ($\triangleq 2a_{[211]}$) and (100) steps of 4-Å width ($\triangleq a_{[110]}$) along $[01\bar{1}]$ thus forming asymmetric pyramides along the $[\bar{1}11]$ direction of 2.3-Å height ($\triangleq 2d_{[211]}$) [Fig. 6(e)].

The RHEED pattern of the (210) surface reveals regular step arrays for observation along the perpendicular [001] [Fig. 7(a)] and $[\bar{1}20]$ directions [Fig. 7(b)]. Similar to the behavior of the (331) surface, the RHEED pattern observed along [001] shows an irreversible roughening of the stepped surface into macroscopic facets above 560 °C. The regular step array is reestablished after the deposition of several GaAs monolayers below 560 °C and is stable during growth. The regular step array observed along the [001] azimuth possesses the lateral periodicity of $l=13$ Å and step height of $h=3.3$ Å. The terrace width w amounts to about $w=7$ Å. The lattice constant a of the terrace plane of 2 Å ($\triangleq \frac{1}{2}a_{[110]}$) identifies the (110) surface configuration in [001] projection. An average domain size of $w=60$ Å is estimated. Observation along $[\bar{1}20]$ reveals the regular step array with a lateral periodicity of $l=5.7$ Å, a step height of $h=2.6$ Å, and a terrace width of about 5 Å. Hence, the (210) surface breaks up into regular step arrays running along [001] and $[\bar{1}20]$. As mentioned above, however, a clear distinction between stepped and faceted surface is not meaningful in this case. The step array with step edges along [001] comprise (110) terraces of 8 Å width ($\triangleq 2a_{[110]}$) and (100) steps of 5.6 Å width ($\triangleq a_{[100]}$). The step array with the step edges along $[\bar{1}20]$ with a lateral periodicity of 5.6 Å ($\triangleq a_{[100]}$) is assigned to (211) terraces and (001) steps. The (211) terraces comprise two lattice constants along $[01\bar{1}]$ and $[\bar{1}11]$. Hence, similar to the surface structure of (211) planes discussed above the (211) terraces here are assumed to be composed of two (111) and one (100) surface configuration. The step arrangement of (210) surfaces finally results in pyramids of 2.5-Å height ($\triangleq 2d_{[210]}$) which are asymmetric along the [001] and $[\bar{1}20]$ directions [Fig. 7(c)].

In summary, the above RHEED investigations of the nonsingular (331), (311), (211), and (210) surfaces representing the three groups of planes between the singular (100), (110), and (111) planes reveal the breaking up of nonsingular planes into macrosteps composed of singular (100), (110), and (111) surface configurations. The various arrangements of macrosteps on the different surfaces comprise (111) faces which are composed of two (111) surface configurations. This behavior shows the important role of the energy minimizing 2×2 surface reconstruction of (111) planes[8] for stabilization of the surface structures on a nanometer scale.

B. RHEED studies of singular surfaces

The RHEED pattern of the singular (110) surface observed along the $[1\bar{1}0]$ azimuth shows a splitting across the integral order streaks into two slashes. In the perpendicular [001] azimuth the streaks are splitted along their length. This intensity distribution is obtained after the deposition of several GaAs monolayers at 480 °C and indicates a periodic step array with the step edges along $[1\bar{1}0]$.[9] The RHEED pattern is stable during growth, however, at temperatures above 480 °C it becomes diffuse, indicating a roughening of the surface. From the splitting across the streaks in the $[1\bar{1}0]$ azimuth, which is clearly seen in the line-shape profiles shown in Figs. 8(a) and 8(b) with enlarged scale, the average lateral periodicity of $l=(90\pm20)$ Å is evaluated. The height h of the steps of about 10 Å is determined from the splitting along the streaks in the [001] azimuth [Fig. 8(c)] using $h=\lambda/\Delta\theta-\theta_{av}l$,[9] where a small inclination of the terrace plane to the (110) surface is assumed due to the large periodicity of the step array. Here, λ is the electron wavelength, $\Delta\theta$ the angular separation of the diffraction peaks (5.5 mrad), and θ_{av} the average final angle corre-

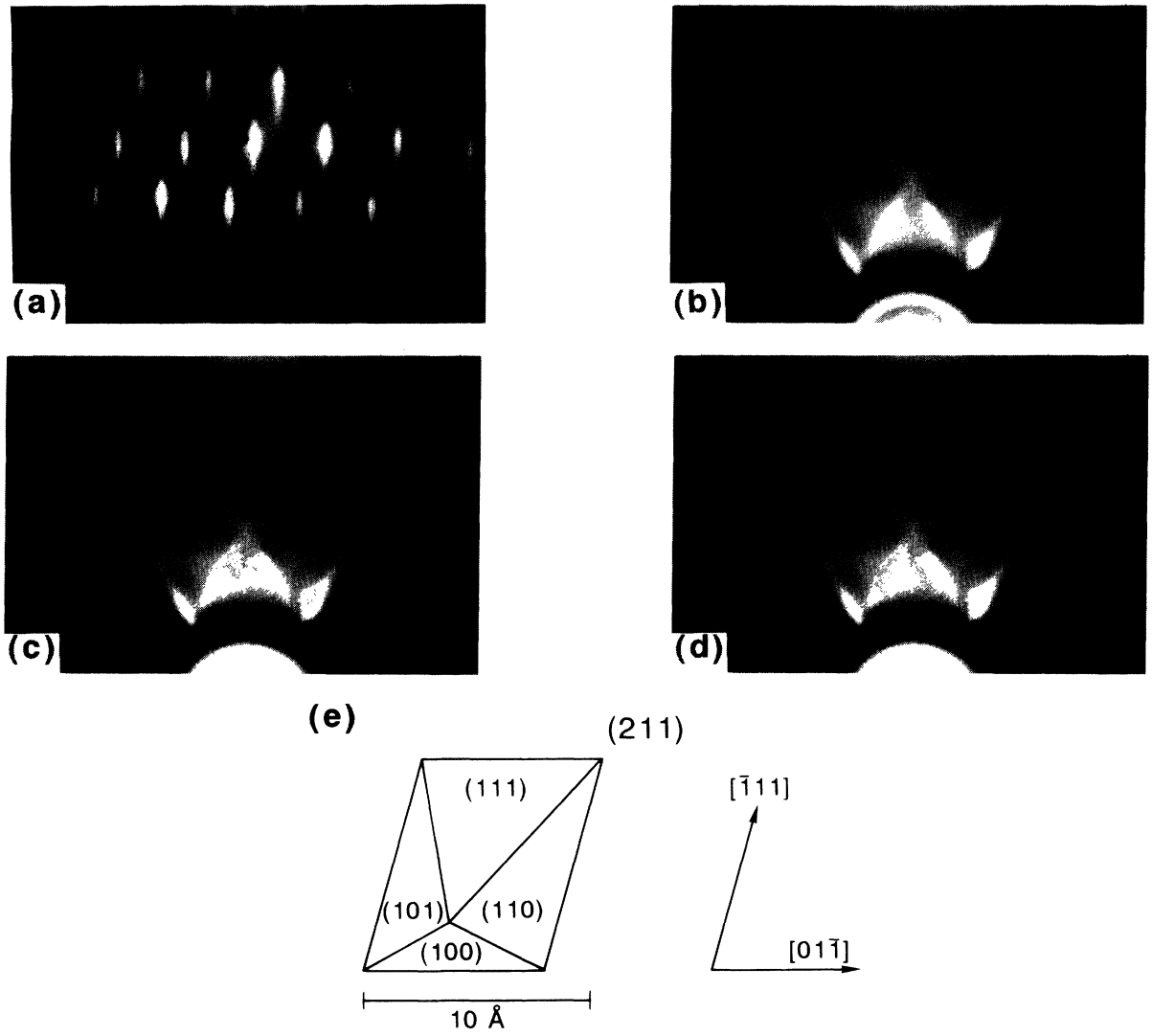

FIG. 6. Reflection high-energy electron diffraction (RHEED) pattern of the GaAs (211) surface taken (a) along $[01\bar{1}]$ and (b) along $[\bar{1}11]$ at 600 °C. (c) and (d) show the RHEED patterns taken along $[\bar{1}11]$ at 570 °C and 520 °C, respectively. (e) Schematic of the stepped surface.

sponding to the n and $n+1$ diffraction peaks (40 mrad). A pronounced degree of fluctuation of the terrace widths of about 30 Å has to be assumed from recent scanning tunneling microscopy investigations of (110) cleavage planes[10] which is also reflected in the line shape of the RHEED intensity profiles [Figs. 8(a) and 8(b)]. Previous investigations of the surface faceting on (110) GaAs epitaxial layers have indicated the step planes to be composed of $(11\bar{1})$ surface configuration.[11] Hence, the (110) surface is described to transform into $(11\bar{1})$ steps of 6.9 Å width, i.e., 4 Å height ($\hat{=}a_{[110]}$), and vicinal (881) terrace planes [Fig. 8(d)]. As in the case of the nonsingular surfaces discussed above, the $(11\bar{1})$ steps here are expected to be stabilized in height by the 2×2 surface reconstruction of (111) planes.

The RHEED patterns of the singular (111) plane show a pronounced splitting along the integral order streaks. This splitting is observed along arbitrary azimuthal directions as shown exemplarily in Figs. 9(a) and 9(b) for the perpendicular $[1\bar{1}0]$ and $[11\bar{2}]$ directions. Hence, this splitting reflects the height of the surface structure of the (111) plane amounting to 13 Å. Splitting across the streaks is not resolved, indicating the lateral periodicity exceeding 100 Å. From the high symmetry of the [111] crystallographic direction, the (111) surface is assumed to break up into symmetric pyramids of 13 Å height ($\hat{=}4d_{[111]}$) built up from vicinal planes.

IV. ELECTRONIC PROPERTIES OF GaAs/AlAs MULTILAYER STRUCTURES

The topography observed on high- and low-index GaAs surfaces is maintained during the growth of GaAs/AlAs multilayer structures indicating the surface structure to be transferred to the GaAs/AlAs heterointerface. This interface corrugation leads to additional la-

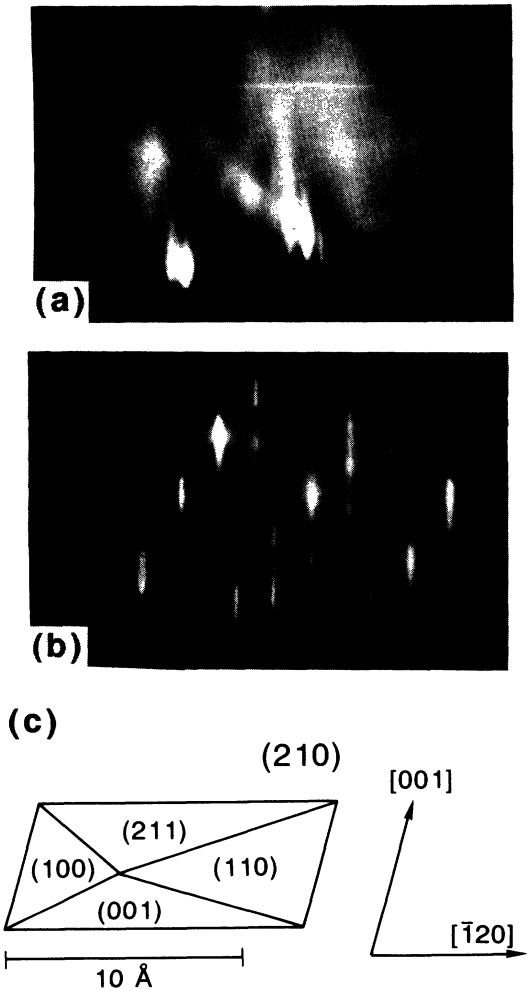

FIG. 7. Reflection high-energy electron diffraction (RHEED) pattern of the GaAs (210) surface taken (a) along [001] and (b) along $[\bar{1}20]$. (c) Schematic of the stepped surface.

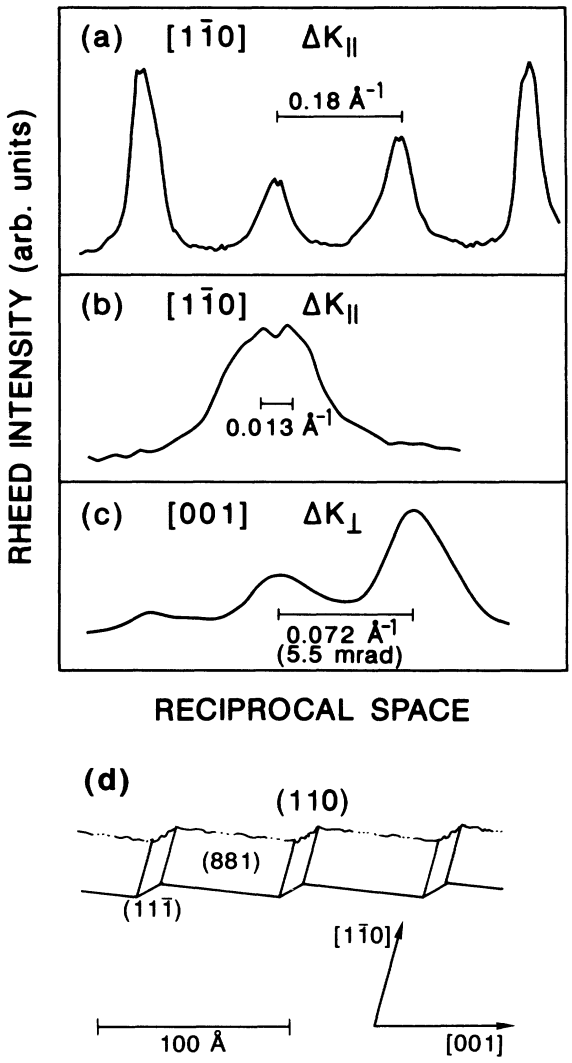

FIG. 8. Reflection high-energy electron diffraction (RHEED) intensity profiles of the GaAs (110) surface measured as a function of the scattering vector $k_{\parallel}$ (a) and (b) along $[1\bar{1}0]$ and (c) as a function of $k_{\perp}$ along [001]. For (c) the angular separation of the diffraction peaks is also indicated. (d) Schematic of the stepped surface.

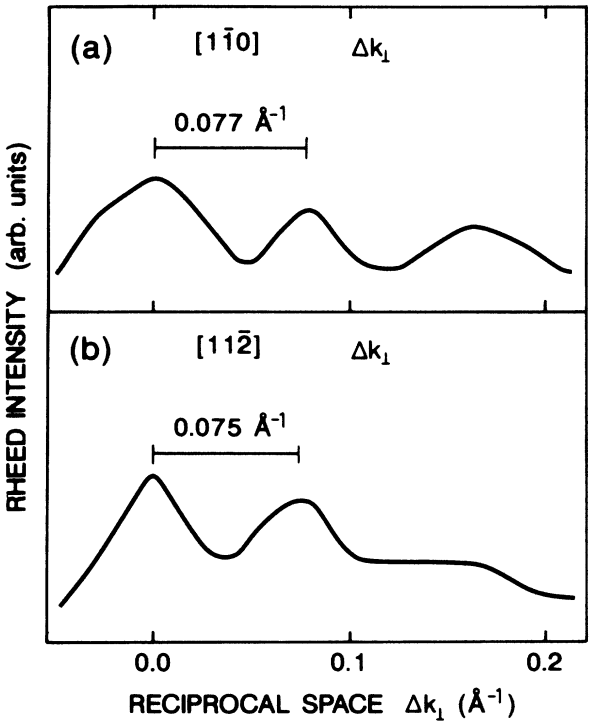

FIG. 9. Reflection high-energy electron diffraction (RHEED) intensity profiles of the GaAs (111) surface measured as a function of the scattering vector $k_\perp$ (a) along [1$\bar{1}$0] and (b) along [11$\bar{2}$].

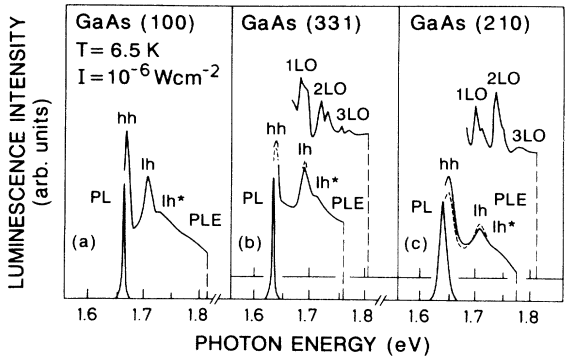

FIG. 10. Photoluminescence (PL) and photoluminescence excitation (PLE) spectra of (a) (100), (b) (331), and (c) (210) GaAs/AlAs multilayer structures. For (b) the solid line is for the exciting light polarized parallel [1$\bar{1}$0] and for (c) parallel [001]. The dashed lines are for the respective perpendicular polarizations. LO and TA phonon related lines are resolved in PLE monitoring the high-energy side of the PL line.

teral confinement effects, i.e., to the formation of GaAs quantum-wire and quantum-dot structures, which is confirmed by the electronic properties of GaAs/AlAs multilayer structures grown on these low- and high-index GaAs substrates.

As the electronic properties of (311) oriented heterostructures have been described in detail in Ref. 12, we concentrate here on the optical properties of GaAs/AlAs multilayer structures grown on (331), (210), and (110) GaAs substrates which are characterized by asymmetric surface structures built up from terrace planes and steps with distinct step sense. Seventy period 48-Å GaAs/50-Å AlAs multilayer structures were grown side by side on (331), (210), (110), and (100) GaAs substrates as reference. The growth temperature was adjusted to 460 °C in order to develop the surface structure for these orientations. The PL line of the (210) structure exhibits a FWHM exceeding those of the (100) and (331) structures revealing the lower degree of ordering of the surface structure of GaAs (210) compared to the (100) and (331) orientations which was clearly seen in the RHEED patterns (Fig. 7). The PL lines and the electron–heavy-hole (*e*-hh) transitions observed in PLE of the (331), (210), and (110) structures exhibit a pronounced redshift compared to the (100) reference sample (Fig. 10 and Table I). This behavior is attributed to the formation of thicker and thinner GaAs and AlAs regions with the luminescence originating from transitions in the respective thicker GaAs regions. The atomic configuration of these asymmetric surface structures suggests the thicker regions to be connected with the steps whereby the thinner regions appear upon the terrace planes. The redshifted *e*-hh transition energies of the (331), (210), and (110) structures correspond to respective GaAs well thicknesses which are about 3 Å thicker than the nominal average GaAs well width for the (331) and (210) structures, and about 5 Å thicker for the (110) structure. These values are in good agreement with the height of the surface corrugation for the different orientations (Table I). We have obtained this result from a finite quantum-well model. The anisotropy of the valence band was taken into account using the hh mass along [110], $m_{\mathrm{hh}[110]}$, and interpolated values be-

TABLE I. Dependence of the redshift of the electron–heavy-hole (*e*-hh) transition and light-hole (lh) exciton continuum energy on the height of the surface corrugation for various orientations.

Orientation	Height of the surface corrugation (Å)	Redshift of the *e*-hh transition (meV)	lh exciton continuum energy (meV)
(100)	0	0	15
(210)	2.5	21	24
(331)	2.6	23	17
(110)	4.0	30	

tween $m_{hh[111]}$ and $m_{hh[110]}$ for $m_{hh[331]}$, and between $m_{hh[100]}$ and $m_{hh[110]}$ for $m_{hh[210]}$ (see Fig. 1). The hh masses along [100] ($m_{hh[100]}=0.34m_0$ for GaAs and $0.75m_0$ for AlAs), along [110] ($m_{hh[110]}=0.57m_0$ for GaAs and $0.87m_0$ for AlAs), and along [111] ($m_{hh[111]}=0.70m_0$ for GaAs and $1.0m_0$ for AlAs) were calculated with the Luttinger parameters taken from Ref. 13 using $m_{hh[100]}=m_0/(\gamma_1-2\gamma_2)$, $m_{hh[110]}=m_0/[\gamma_1-(\gamma_2^2+3\gamma_3^2)^{1/2}]$ and $m_{hh[111]}=m_0/(\gamma_1-2\gamma_3)$. The conduction-band offset was set to $\Delta E_c=0.60\Delta E_{gap}$ (Ref. 14) with the direct band-gap energies of GaAs [E_{gap}(GaAs)=1.52 eV] and AlAs [E_{gap}(AlAs)=3.13 eV] taken from Ref. 15. The appearance of strong LO and TA phonon related lines in the PLE spectra monitoring the high-energy side of the luminescence from the (331), (210), and (110) samples (not shown here) exhibits enhanced exciton phonon interaction and increased exciton stability due to the lateral localization and shrinkage of the exciton diameter in the interface corrugation which favors the excitons created above the band gap relaxing as a whole.[12,16,17] The high stability of the excitons is further revealed in the enhancement of the light-hole (lh) exciton continuum energies (lh*) observed in the PLE spectra (Fig. 10 and Table I) which is even more pronounced for the (210) sample where the interface corrugation is effective in two directions. The lh exciton continuum energy was not resolved for the (110) sample. The pronounced optical anisotropy shown in Fig. 10 for the (331) and (210) samples is in agreement with the lateral potential introduced by the interface structure for these orientations.[18]

V. CONCLUSION

In conclusion we have investigated the surface structure of the nonsingular (331), (311), (211), and (210) GaAs surfaces representing the three group of planes between the singular (100), (110), and (111) planes, and on the singular (110) and (111) GaAs surfaces. RHEED directly reveals the formation of a variety of surface structures on the different planes during MBE. Nonsingular planes break up into singular surface configurations, whereas the singular planes transform into vicinal surfaces. Surface reconstruction plays an important role in stabilizing the observed surface structures on a nanometer scale. These surface structures provide a unique means to directly synthesize quantum-wire and quantum-dot structures which is confirmed by the observed distinct electronic properties of GaAs/AlAs multilayer structures.

ACKNOWLEDGMENTS

We like to thank H. P. Schönherr and A. Fischer for expert help with the MBE growth. Part of this work was sponsored by the Bundesministerium für Forschung und Technologie of the Federal Republic of Germany.

*Present address: Paul-Drude-Institut für Festkörperelektronik, O-1086 Berlin, Federal Republic of Germany.

†Present address: Department of Materials Science, Technical University, D-6100 Darmstadt, Federal Republic of Germany.

[1]E. D. Williams and N. C. Bartelt, Science **251**, 393 (1991).

[2]B. Z. Olshanetsky and V. I. Mashanov, Surf. Sci. **111**, 414 (1981).

[3]D. W. Shaw, IOP Conf. Proc. No. 7 (Institute of Physics and Physical Society, London, 1969), p. 50.

[4]R. C. Sangster, in *Compound Semiconductors Vol. I,* edited by R. K. Willardson and H. L. Goering (Reinhold, New York, 1962), p. 241.

[5]H. Fronius, A. Fischer, and K. Ploog, Jpn. J. Appl. Phys. **25**, L137 (1986).

[6]M. Henzler, Appl. Surf. Sci. **12**, 450 (1982).

[7]M. G. Lagally, D. E. Savage, and M. C. Tringides, in *Reflection High-Energy Electron Diffraction and Reflecting Electron Imaging of Surfaces,* Vol. 188 of *NATO Advanced Study Institute, Series B: Physics,* edited by P. K. Larsen and P. J. Dobson (Plenum, New York, 1988), p. 139.

[8]S. Y. Tong, G. Xu, and W. N. Mei, Phys. Rev. Lett. **52**, 1693 (1984).

[9]P. R. Pukite, J. M. van Hove, and P. I. Cohen, J. Vac. Sci. Technol. B **2**, 243 (1984).

[10]Y. N. Yang, B. M. Trafas, R. L. Siefert, and J. H. Weaver, Phys. Rev. B **44**, 3218 (1991).

[11]L. T. Allen, E. R. Weber, J. Washburn, and A. G. Elliot, J. Cryst. Growth **87**, 193 (1988).

[12]R. Nötzel, N. N. Ledentsov, L. Däweritz, K. Ploog, and M. Hohenstein, Phys. Rev. B **45**, 3507 (1992).

[13]L. W. Molenkamp, R. Eppenga, G. W.'t Hooft, P. Dawson, C. T. Foxon, and K. J. Moore, Phys. Rev. B **38**, 4314 (1988).

[14]D. F. Nelson, R. C. Miller, and D. A. Kleinman, Phys. Rev. B **35**, 7770 (1987).

[15]O. Madelung, in *Numerical Data and Functional Relationships in Science and Technology,* edited by O. Madelung, Landolt-Börnstein, New Series, Group III, Vol. 22a, Pt. 2 (Springer-Verlag, Berlin, 1986), p. 84.

[16]S. Permogorov, Phys. Status Solidi B **68**, 9 (1975).

[17]J. J. Hopfield, J. Phys. Chem. Solids **10**, 110 (1959).

[18]D. S. Citrin and Y. C. Chang, Phys. Rev. B **43**, 11 703 (1991).

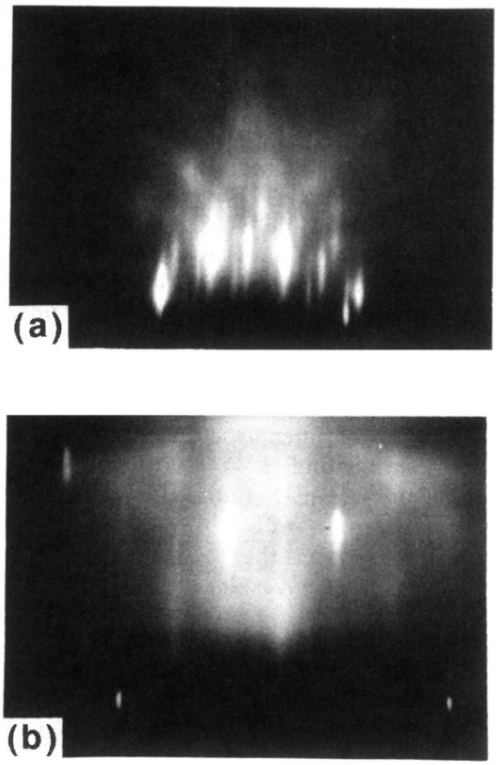

FIG. 4. Reflection high-energy electron diffraction (RHEED) pattern of the GaAs (331) surface taken (a) along [1 $\bar{1}$0] and (b) along [$\bar{1}$ $\bar{1}$6]. (c) Schematic of the stepped surface.

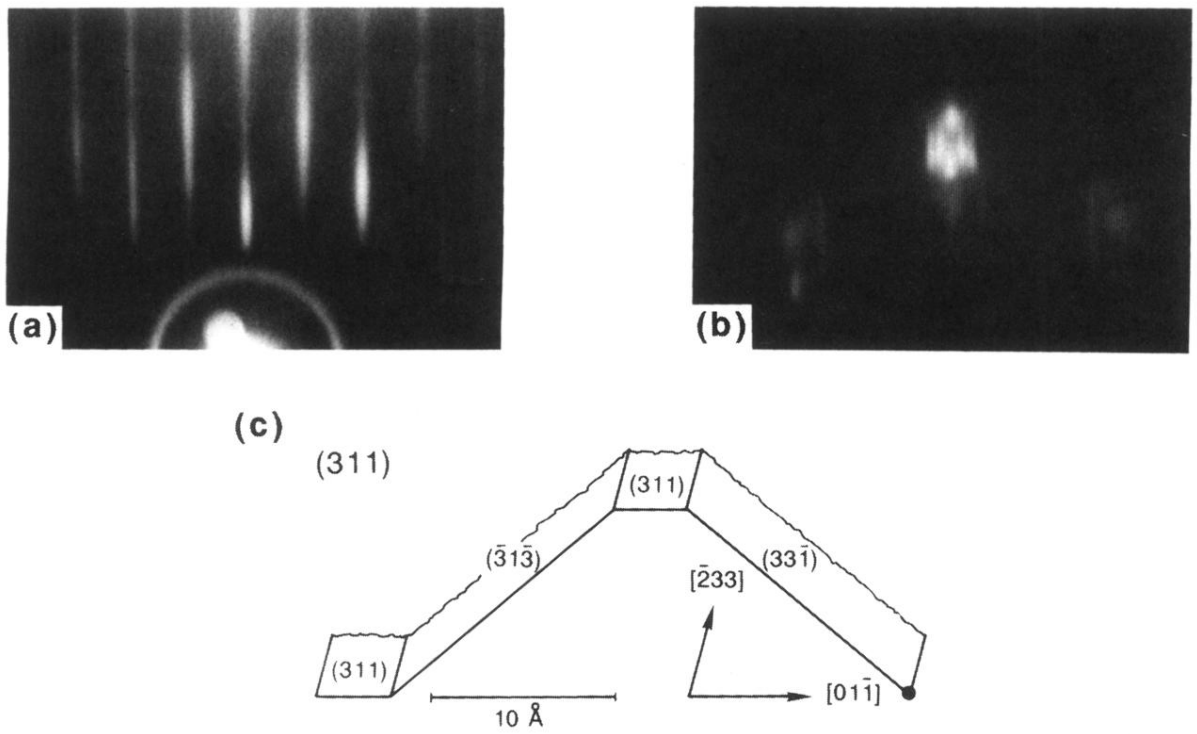

FIG. 5. Reflection high-energy electron diffraction (RHEED) pattern of the GaAs (311) surface taken (a) along $[01\bar{1}]$ and (b) along $[\bar{2}33]$. (c) Schematic of the stepped surface.

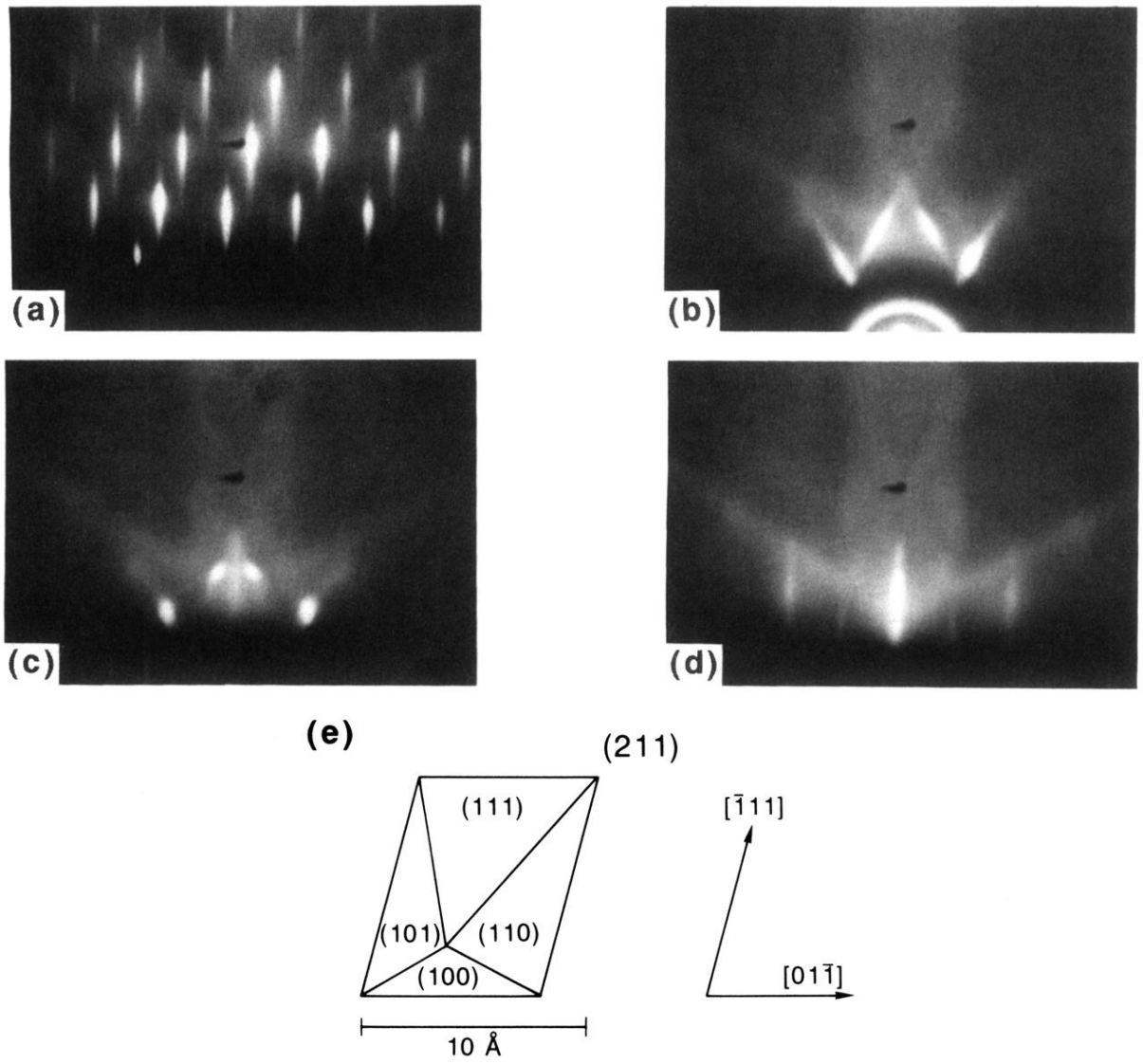

FIG. 6. Reflection high-energy electron diffraction (RHEED) pattern of the GaAs (211) surface taken (a) along [01$\bar{1}$] and (b) along [$\bar{1}$11] at 600 °C. (c) and (d) show the RHEED patterns taken along [$\bar{1}$11] at 570 °C and 520 °C, respectively. (e) Schematic of the stepped surface.

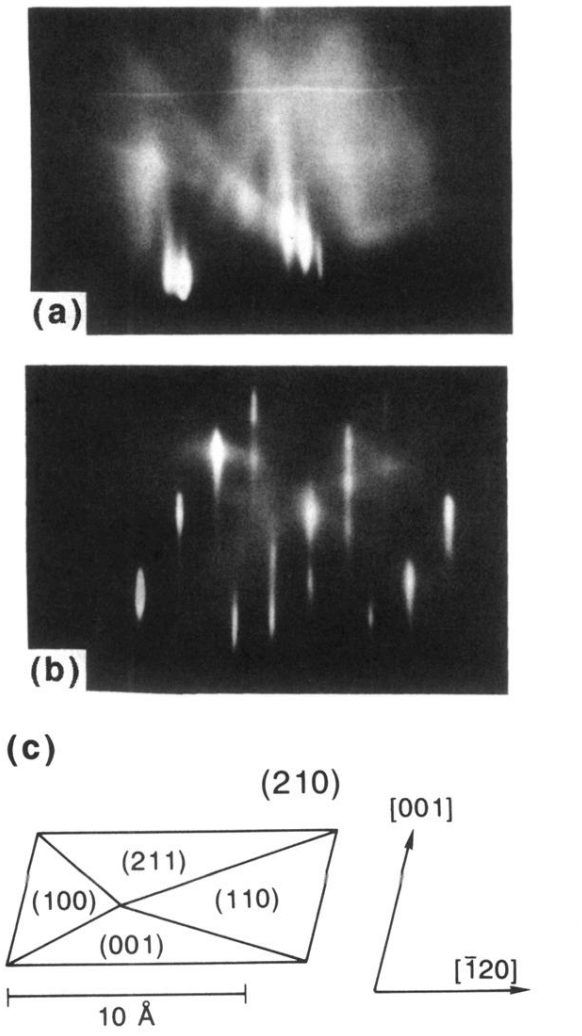

FIG. 7. Reflection high-energy electron diffraction (RHEED) pattern of the GaAs (210) surface taken (a) along [001] and (b) along [$\bar{1}$20]. (c) Schematic of the stepped surface.